Effects of Aging on Human Meibum

Igor A. Butovich[1,2] and Tomo Suzuki[3,4]

[1]Department of Ophthalmology, University of Texas Southwestern Medical Center, Dallas, Texas, United States
[2]The Graduate School of Biomedical Sciences, University of Texas Southwestern Medical Center, Dallas, Texas, United States
[3]Department of Ophthalmology, Kyoto Prefectural University of Medicine, Kyoto, Japan
[4]Department of Ophthalmology, Kyoto City Hospital Organization, Kyoto, Japan

Correspondence: Igor A. Butovich, Department of Ophthalmology, and The Graduate School of Biomedical Sciences, University of Texas Southwestern Medical Center, 5323 Harry Hines Boulevard, Dallas, TX 75390, USA; igor.butovich@utsouthwestern.edu.

Received: July 8, 2021
Accepted: August 15, 2021
Published: September 21, 2021

Citation: Butovich IA, Suzuki T. Effects of aging on human meibum. *Invest Ophthalmol Vis Sci.* 2021;62(12):23. https://doi.org/10.1167/iovs.62.12.23

Purpose. The purpose of this study was to determine if aging affects meibum lipid composition in non-meibomian gland dysfunction (MGD)/non-dry eye (DE) population. Aging has been repeatedly linked to pathological changes in various tissues and organs, including the onset of MGD and DE, in a number of clinical and population-wide surveys. Both conditions have been associated with abnormal meibum secretion and composition, among other factors. However, the chemical basis for such a connection has not been established yet.

Methods. To identify and characterize possible changes in the meibum and meibogenesis with aging, lipidomic analyses of meibum samples collected from human subjects of two age groups – young (29 ± 5 years, $n = 21$) and elderly (68 ± 7 years, $n = 29$) – with similar male to female ratios in each group were conducted. Intact lipid species from major lipid groups of meibum (such as wax esters, cholesteryl esters, free cholesterol, triacylglycerols, etc.) were compared using lipidome-wide untargeted (such as Principal Component Analysis) and targeted (such as Orthogonal Projections to Latent Structures Discriminant Analysis) approaches, along with focused analyses of specific lipid species in liquid-chromatography mass spectrometry (LC-MS) and tandem mass spectrometry (MS-MS) experiments.

Results. Extremely high similarities of meibum lipids in the two age groups were observed, with only minor changes in the individual lipid species. The magnitude of the intergroup variability for tested lipid species was comparable to the intragroup variability for the same meibum components. No statistically significant differences in the lipid esterification, elongation, and unsaturation patterns were observed.

Conclusions. Chronological aging itself seems to have only minor effect on meibogenesis in healthy, non-MGD/non-DE subjects.

Keywords: meibum, meibomian glands, aging, lipidomics, chromatography, mass spectrometry

In previous studies, aging has been repeatedly associated with the onset of dry eye (DE) and meibomian gland dysfunction (MGD) in humans.[1–3] A significant number of publications reported that DE (in its evaporative form) and MGD are related to changes in either quantity or quality of meibum produced by meibomian glands (MGs). The adverse changes in the quantity of produced meibum can be either of hyposecretory or hypersecretory nature.[4] The former is, typically, associated with either MG dropout, which is a common, age-related abnormality that is described as MG atrophy resulting in partial or complete arrest of meibum production,[5] or MG obstruction – a blockage of MG orifices and/or ducts that impede meibum delivery from the glands onto the ocular surface,[6] or both.[7] The hypersecretory form of MGD,[8] on the other hand, may be related to either MG hypertrophy or higher expressibility of meibum. The quality (i.e. composition) of meibum can also change in response to adverse effects of inflammation (such as in chalazia[9,10]), systemic lipid disorders, as demonstrated in a mouse model,[11] and, possibly, diet.[12]

Although the effects of aging on MG morphology and physiology have been reported before, information on its possible association with actual biochemical changes in meibum is scarce. Most of existing reports came from studies that utilized infrared spectrometry (IR) and nuclear magnetic resonance spectroscopy (NMR), to characterize differences between meibum samples collected from donors of different ages.[13–19] Although difficult to quantitate, major conclusions that were drawn from those studies were: (1) a two-fold shortening of the overall length of meibomian lipids with aging, and (2) a concomitant, also two-fold, increase in their degree of unsaturation. The first conclusion was based on an estimate of the overall ratio of terminal (end) alkyl CH_3 groups to internal methylene CH_2 groups, whereas the second – on the increase in the number of double bounds in meibomian lipids, which both went up with aging. Also

reported were relative increases in the cholesteryl esters (CEs),[18] a decrease in lipid peroxidation in meibum of patients with MGD,[15] and, controversially, its increase in the tears of the elderly,[20] detected chromatographically measuring malondialdehyde – a marker of lipid peroxidation.

Notwithstanding the importance of these observations, it needs to be emphasized that changes in many parameters measured by IR and/or NMR in complex lipid mixtures (such as the meibum) cannot be attributed to any specific lipid, group of lipids, or even a specific lipid class, and, thus, to any specific subpathways of meibogenesis.[21,22] Indeed, neither NMR nor IR can differentiate between wax esters (WEs), (*O*)-acyl-ω-hydroxy fatty acids (OAHFA), CEs of OAHFA (Chl-OAHFA), and diacylated α,ω-diols (DiAD) in a mixture as these lipid classes have identical groups/bonds, such as esters [–$(CH_2)_n$−C(O)−O−$(CH_2)_n$−], terminal methyl and methylene groups [CH_3−$(CH_2)_n$−], and dienes [−CH_2−CH=CH−CH_2−], and so do CEs and Chl-OAHFA which share [−$(CH_2)_n$-C(O)–O−Chl, CH_3−$(CH_2)_n$−] and diene groups. Thus, it remained unclear which groups of lipids were affected, and which genes, enzymes, and receptors should be targeted to alleviate the effects of aging on MG and meibogenesis.

A more appropriate liquid chromatography-mass spectrometry (LC-MS) approach was used in another earlier study[23] to determine the effects of aging on polar and neutral lipids in human meibum. However, the main conclusion drawn from those experiments that both groups of lipids were adversely affected by aging, was based on erroneous lipid characterization: The mass-to-charge ratio (unitless) (*m/z*) values of "neutral lipids" reported in that study (between 110 and 150; table 3 and figure 3, *ibid.*) as analyte identifiers could not possibly belong to any lipid, as even shortest neutral lipids – WE and CE – would produce the *m/z* values in the 400 to 800 range. The data on "polar lipids" (table 2; *ibid.*) show changes in a group of MS signals with *m/z* values varying from 163 to 873, none of which could be attributed to any known lipid species as no authentic standards were used to verify their structures, no LC retention times were determined, no tandem mass spectrometry (MS/MS) fragmentation patterns for any analyte were produced, and no high resolution *m/z* values that would be sufficient for elemental analyses were reported, meaning that the goals of the study remained largely unattained.

Thus, the actual molecular basis for a connection between DE/MGD and quality of meibum has not been firmly established yet, and it is still unknown how, or even if, aging affects meibum in the non-MGD/non-DE population. To provide an insight into the possible changes in meibomian lipid homeostasis with aging, in the current study, we compared the meibum of young adults and the elderly using a combination of ultra-high performance LC and high resolution MS.

Materials and Methods

Reagents

Lipid standards were obtained from Sigma-Aldrich (St. Louis, MO, USA) and Nu-Chek Prep., Inc. (Elysian, MN, USA). HPLC or MS grade organic solvents (iso-propanol [IPA], acetonitrile [AcN], methanol [MeOH], chloroform [$CHCl_3$], and water) and ammonium formate (99.98%) were obtained from Sigma-Aldrich, Burdick & Jackson (Muskegon, MI, USA), and Thermo Fisher Scientific (Waltham, MA, USA). Ultra-high pure nitrogen was used for sample preparation.

LC-MS Equipment

A Synapt G2-Si quadrupole time-of-flight mass spectrometer, a Zspray housing, IonSabre-II atmospheric pressure chemical ionization (APCI) ion source, a LockSpray unit, a binary Acquity M-Class chromatograph with an autoinjector, C18 BEH (1 × 100 mm, 1.7 µm) and C8 BEH (2.1 × 100 mm, 1.7 µm) columns were from Waters Corp. (Milford, MA, USA).

Human Subjects and Collection of Meibum Samples

The volunteers were recruited at the University of Texas Southwestern Medical Center in Dallas (UTSWMC, Dallas, TX, USA), Kyoto Prefectural University of Medicine (KPUM, Japan), and the affiliated Kyoto City Hospital (KCH, Japan). Collection procedures were approved by the Institutional Review Boards at UTSW, KPUM, and KCH. Young (20–35 year old) and elderly (60–90 year old) healthy subjects with no symptoms consistent with MGD or DE were selected for this study. Volunteers were recruited from the local population in Kyoto, Japan, and Dallas, Texas. Exclusion criteria for Asian volunteers were as follows: anatomic and/or functional abnormality of eyelids, ocular allergies, history of eye surgery, contact lens wear, antiglaucoma treatment, and continued use of local or systemic antimicrobial or steroid medication. After signing informed consent forms, volunteers were treated in accordance with the tenets set forth in the Declaration of Helsinki. Both eyes of each patient were examined using a slit-lamp microscope. Lid-margin abnormality (vascularity, displacement of the mucocutaneous junction, and irregularity) and obstruction of MG orifices, such as plugging, were evaluated according to Japanese MGD diagnostic criteria.[24] The tear film breakup time (FBUT) was measured three times consecutively after the instillation of fluorescein and the median value was adopted. Reduced meibum expression in response to moderate digital pressure was scored from 0 to 3.[25] Meiboscores for upper and lower eyelids were determined using noncontact meibography and assigned values from 0 to 3.[26] All volunteer subjects in this study did not meet either Japanese MGD diagnostic criteria[24] or DE criteria (FBUT ≤5 seconds).[27] Less scored eye was selected for meibum collection. Therefore, the meibum was collected from both upper and lower eyelids of one eye. When there were no differences in the score, the right eye was selected for meibum collection. In the United States, eligible donors underwent similar ocular examination as described earlier.[28] After cleaning the eyelid rims with cotton swabs and numbing the ocular tissues with a few drops of proparacaine, meibum samples were collected using gentle expression from the eyelids and platinum microspatulas.[28] Meibum specimens were dissolved and stored in small volumes (typically, 1 mL) of $CHCl_3$/MeOH = 3:1 (v/v) solvent mixture in sealed glass HPLC autoinjector vials at −20 to −80°C before further processing.

The age and sex distribution of study subjects is shown in the Table. None of the donors had a history of DE or MGD. Some elderly donors displayed minor to mild age-related MG dropout.

Table. Human Study Subjects

Subject Group	Number of Subjects	Race, Asians/Caucasians*	Age (Mean ± Standard Deviation)	M/F
Y	22†	18†/4	29 ± 5	10/12
E	29	18/11	68 ± 7	13/16

* In a previous study, race was shown to have virtually no effect on meibogenesis.[29]
† One of the Asian samples from the Y group was later classified as an outlier with low abundance of Meibomian lipids and high contaminations and was treated with caution.

Analytical Procedures

Before the analyses, the solvent was evaporated from the samples under a stream of nitrogen and the oily/waxy residue was redissolved in a small volume (typically, 1 mL) of IPA. The samples were centrifuged at 1000 g for 1 minute and then analyzed by LC-MS, as described before.[29,30] Depending on the concentration of the sample, between 0.3 and 1 µL of its stock solution in IPA was injected.

Two types of chromatographic columns – C8 and C18 – were used to analyze meibum samples. The C8 column was used in combination with isocratic elution of the analytes in a 95% IPA: 5% 10 mM ammonium formate in water solvent mixture (IPA95) at a flow rate of 20 µL/min and a temperature of 35°C. All analytes eluted between 12 and 20 minutes of a 25-minute long run. This approach minimized dilution of the analytes and resulted in a condensed chromatogram with rather high ion counts, still offering some chromatographic separation of the lipids (e.g. free cholesterol [Chl] and CE), and removal of polar contaminants (not shown).

The C18 column, on the other hand, was used in combination with a linear gradient of AcN and IPA (both with 5% of 10 mM aqueous ammonium formate) at the same flow rate and temperature.[28,29] The length of the experiment, including the washing and equilibration steps, was 75 minutes. This approach led to an almost baseline separation of a large number of lipids (which was important to discriminate between isobaric analytes), albeit at the expense of lower sensitivity of the analyses due to increased dilution of the samples.

In both cases, the effluent was channeled to the APCI ion source for detection of lipids in positive and negative ion modes (PIM and NIM, correspondingly). In PIM, the lipids were detected mostly as proton adducts, although exceedingly minor amounts of potassium, sodium, and ammonium adducts were also detected for some lipids. In NIM, acidic analytes were seen as anions of different nature, typically of $(M–H)^-$ type. The samples were simultaneously analyzed in MS and MS^E modes with Leucine-Enkefalin as a LockSpray reagent.

Data Processing

Initially, the raw files were imported in Progenesis QI software (from Waters Corp.) and processed to determine a reference run. In pilot experiments with a C8 column, all analytes eluted between 12 and 20 minutes into the run. Therefore, the ions beyond this range were not included in the analysis. The $(M + H)^+$, $(M + K)^+$, $(M + Na)^+$, $(M + NH_4)^+$, and $(M + H - H_2O)^+$ adducts were initially considered as expected analytical ions. However, in most cases only $(M + H)^+$, $(M + K)^+$, and $(M + H - H_2O)^+$ adducts were detected above the 0.02% of the largest peak in a spectrum. Other ions were either not detected, or detected at very low levels that precluded them from reliable quantitation. The data were normalized using total ion abundances in each run. To compensate for inadvertent spikes in chromatograms, a minimum LC-MS peak width for these calculations was set to be 0.5 minutes. After peak picking, the compound statistics was calculated using unsupervised PCA approach. Then, the data were exported to the EZinfo software package (version 3.0.3.0; from Umetrics; a part of Progenesis QI software package) and further analyzed using its built-in Principal Component Analysis (PCA-X) and Orthogonal Projections to Latent Structures Discriminant Analysis (OPLS-DA) templates.

For targeted lipidomic profiling, the LC-MS data were processed in MassLynx software package. Extracted ion chromatograms (EICs) for each of specific *m/z* values were generated from the raw LC-MS files using 50 mDa window, smoothed (if needed) and integrated to determine the LC peak areas. The *m/z* values, obtained at 40,000 FWHM resolution and better than 10 mDa accuracy (typically, 1 to 7 mDa), were used to calculate the elemental composition of the analytes using the EleComp routine of the MassLynx software package. The data were obtained for all indicated analytes and compared using Student's *t*-test for two groups, Y and E. This targeted approach proved to be rather laborious, but necessary to verify the data obtained using the PCA-X and OPLS-DA approaches.

Results

Untargeted Lipidomic Analysis of Meibum Samples

The chemical complexity of meibum[21,31,32] makes side-by-side comparisons of specimens of different origin to find commonalities and differentiating features challenging. Therefore, we used the PCA-X approach that required neither a prior knowledge of the chemical nature of the analytes, nor a list of specific targets for the analyses. As a first step in untargeted comparison of meibum specimens collected from young and elderly subjects, the samples were analyzed using isocratic reverse phase chromatography on a C8 column with the IPA95 eluent and APCI MS detection of the analytes in PIM (Fig. 1A). A high-resolution observation mass spectrum of a representative sample is shown in Figure 1B. As some of the signals were stronger than the others, a section of the spectrum from *m/z* 750 to *m/z* 1,300 with weaker signals was magnified × 125 for clarity. Major lipid components of human meibum were characterized in our previous studies whose results have been summarized in several review papers,[21,32–34] and by other researchers.[35–37] For readers' convenience, a list of most prominent meibomian lipids with their corresponding *m/z* values is shown in Supplementary Table S1.

The following steps for data analysis were taken. First, the raw LC-MS data were imported into the Progenesis QI software package and processed, as described in the

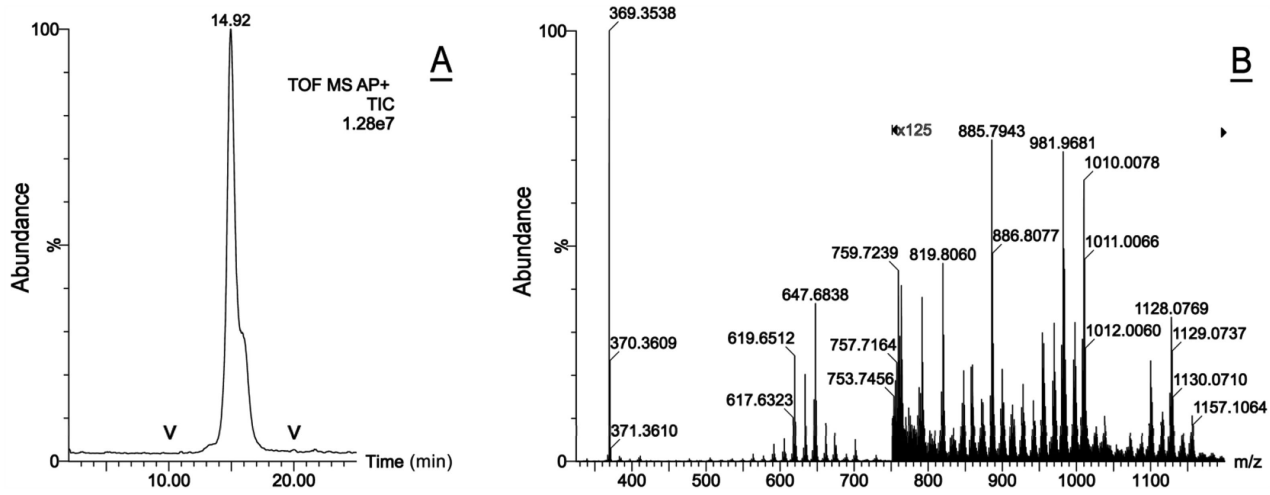

Figure 1. C_8-LC/APCI PIM MS analysis of a representative sample of human meibum. (**A**) Total ion chromatogram. (**B**) Observation spectrum of the sample obtained by combining all spectra recorded from 10 to 20 minutes as labeled in **A**. The *m/z* range from 750 to 1,300 in **B** was magnified × 125 for clarity because of the low abundance of ions.

Materials and Methods section. The initial analysis of 21 Y and 29 E samples resulted in a dataset of 50 observations (i.e. samples, all included with no rejects). The dataset was filtered to include all ions with intensities of more than 0.02% of the base peak and a peak width of 0.5 minutes and above (to exclude sporadic noise), which resulted in 393 variables (i.e. analytes with unique combinations of LC retention times and *m/z* values). Then, the data was normalized using total ion abundance as a common denominator. Most of the ions (~86%) were $(M + H)^+$ adducts, with $(M + K)^+$ being a distant second (~11%). Products of spontaneous in-source dehydration $(M - H_2O + H)^+$ accounted for ~2% of all ions, whereas $(M + Na)^+$ ions were present at ~0.7%. Ammonium adducts were found at ~0.2%, which was barely above the noise level.

Then, the data were exported to EZinfo software for further analyzing. Initially, the data were overviewed using the PCA-X model for a nondiscriminate cluster analysis. The following scores plot was generated (Fig. 2A) using Pareto scaling with no transformation of the data and 8 components that explained 86% of the variance R2X(Cum) (Fig. 2B). One can see that the Y and E samples produced no clearly separated groups with just two mild outliers laying beyond the Hotelling's ellipse (95%) with R2X[1] and R2X[2] statistics values (0.3159 and 0.1613, respectively) that indicated only minor inter- and intragroup differences. The Hotelling's T2 Range plot (Fig. 2C) also demonstrated a comparable spread (i.e. intragroup variability) of Y and E samples and lacked any strong outliers, with all samples grouping at, or below, the T2 Crit (95%) level. Further analysis with the DModX tool produced a graph with just one moderate outlier and two samples barely exceeding D-Crit (99%) threshold (Fig. 2D).

Next, loadings were evaluated. The loadings plot (Fig. 2E) revealed noticeable impacts of WE with *m/z* values of 619.6392, 633.6548, and 647.6704, and a combined signal of CE (ions *m/z* 369.3519), which were positioned farthest from the center of the graph. Other variables (e.g. ions *m/z* 591.6073, 605.6231, 563.5758, and 577.5900) that grouped in the lower left quarter of the graph, also affected the separation of the samples. The fold changes, and their statistical significance, of a fourth group of variables – lipids with *m/z* values of 661.6853, 673.6856, 689.7140, 701.7168, and 1009.9868, and some others – were smaller than those that were mentioned above, and so were parameters for ions *m/z* 589.5920, 549.5607, 535.5451, and 521.5294 (all WE). The rest of the variables were tightly grouped around the center of the graph and had only minor impact on the scores. These groups of lipids represented several clusters of potential biomarkers that differentiated E and Y samples, with ions positioned farthest from the center of the graph and its axes contributing most to the separation of study populations.

Targeted Analyses of Meibum Samples

Then, the data were analyzed using a discriminate OPLS-DA routine of the Progenesis QI and Pareto scaling with no transformation (Fig. 3A). The scores plot showed only a modest separation between the groups with E and Y samples grouping on the left and the right halves of the graph, correspondingly. The intragroup differences between the samples were of the same magnitude as their intergroup differences with only a rather small R2XCum[1] value of 0.2612. Note that some of the E samples overlapped with Y samples in the right quarters of the plot. With the exception of one sample, no strong outliers were detected among the rest 49 samples that were residing within the 95% Hotelling's T2 ellipse. A Hotelling's T2 Range plot revealed no strong outliers either (Fig. 3B).

One of the most informative and useful transformations that is used in multivariate OPLS-DA analysis is the S-Plot (Fig. 3C), which provides visual and quantitative information on loadings and their characteristics which are required for identification of potential biomarkers and discriminating factors in general. One can see that several groups of signals in the upper right and lower left quarters of the graphs had strong and statistically significant impacts on the separation of the sample groups. Signal pairs with *m/z* values of 1128.0660/759.7222 and 1156.0958/787.7535 were identified in earlier studies as major meibomian Chl-OAHFA and their OAHFA fragments,[38–40] whereas signals *m/z* 605.6231, 631.6379, 633.6548, 659.6681, and 661.6853 are of WE nature.[41] Variables with *m/z* 619.6392, 701.7168, and 729.7455 that also belong to the class of WE, on the

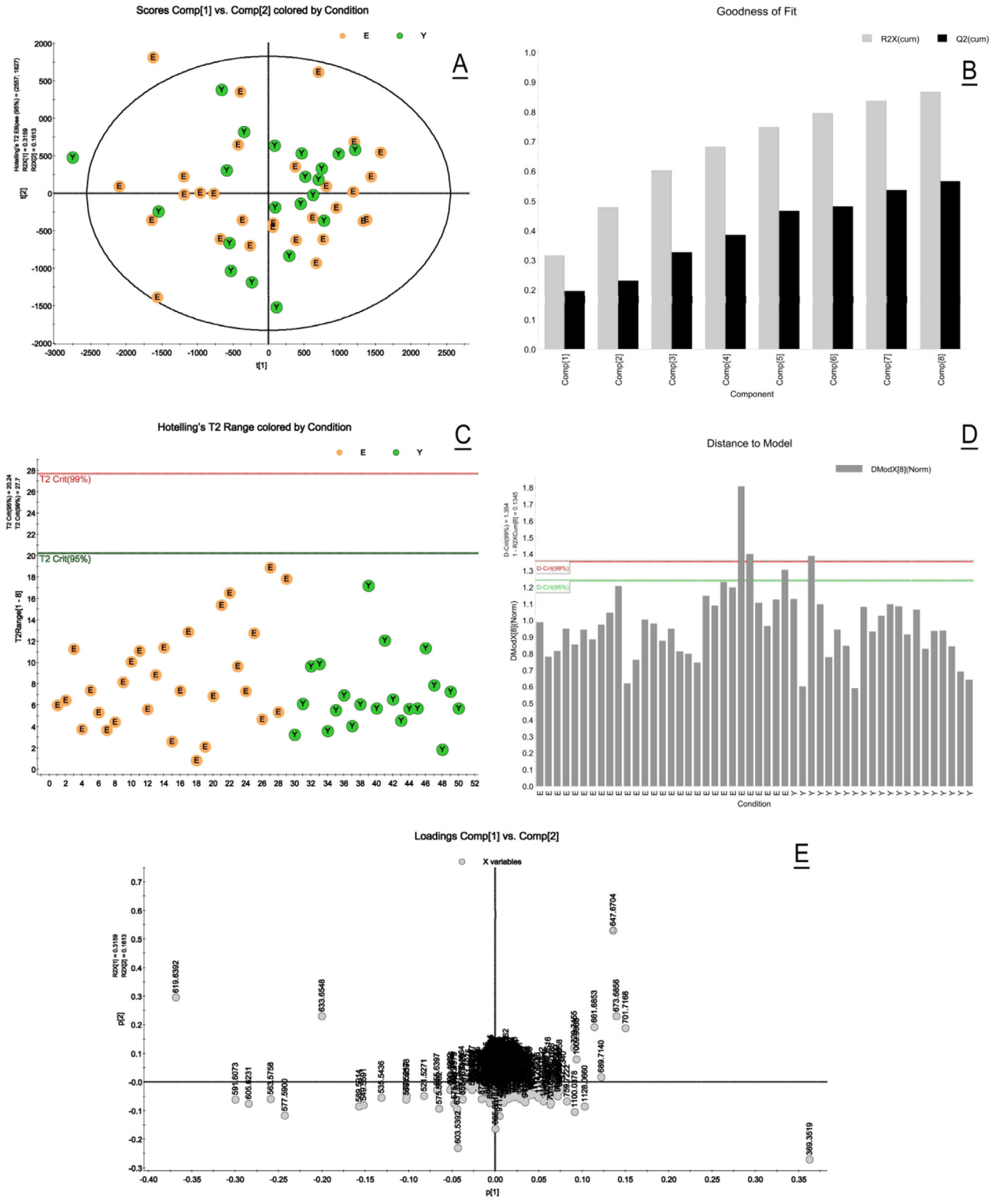

Figure 2. A PCA-X analysis of E and Y human meibum samples. (**A**) A PCA-X scores plot of 21 Y and 29 E human meibum samples analyzed in a LC-MS experiment. (**B**) A PCA-X Goodness of Fit plot of 21 Y and 29 E human meibum samples. Eight component model explained 86% of sample variance. (**C**) A PCA-X Hotelling's T2 Range plot produced no strong outliers that would fall above the T2 Crit (95%) limit. (**D**) A PCA-X Distance-to-Model plot of 29 E samples (bars 1–29) and 21 Y samples (bars 22–50). (**E**) A PCA-X loadings plot of 21 Y and 29 E human meibum samples analyzed in a LC-MS experiment.

Investigative Ophthalmology & Visual Science

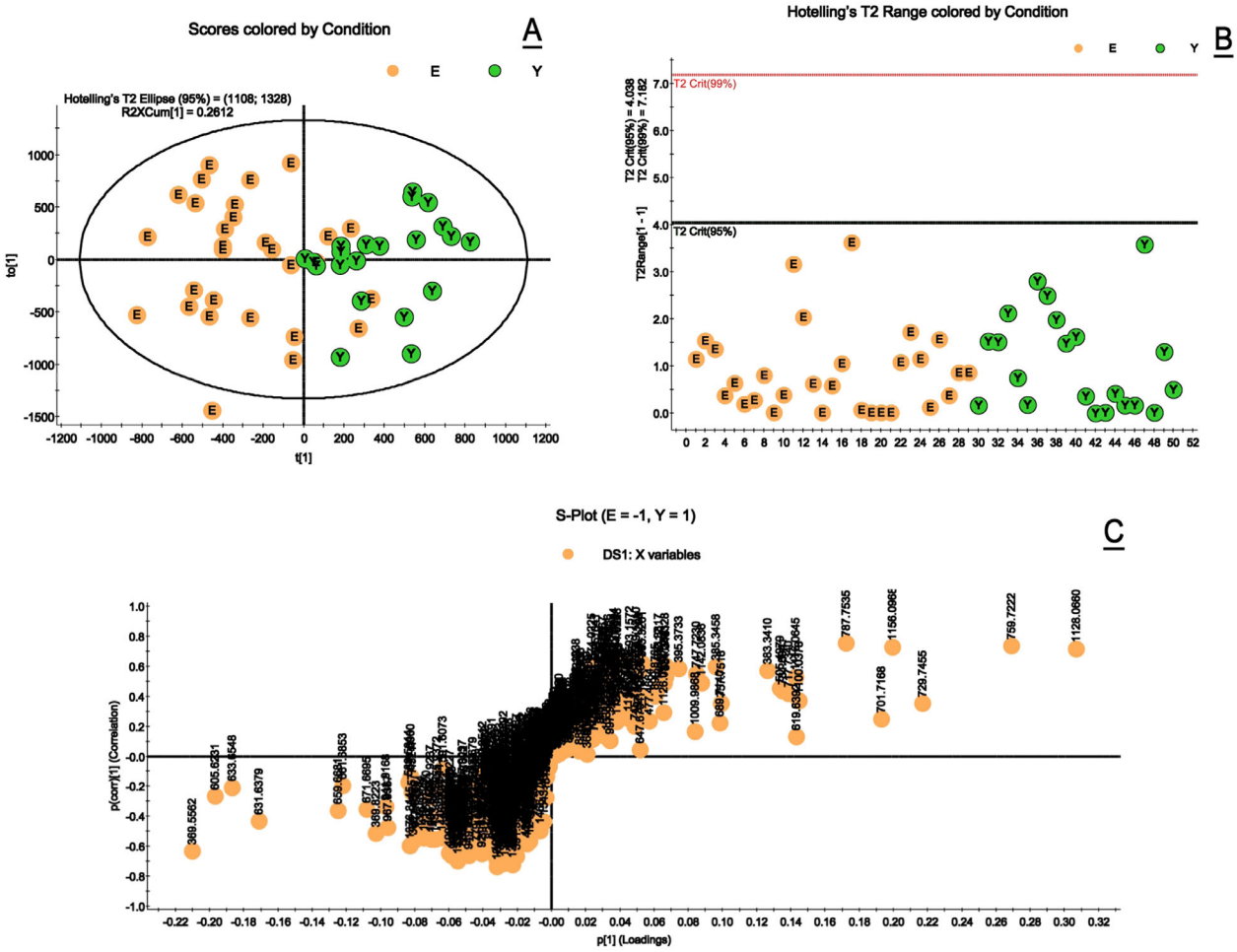

Figure 3. Targeted OPLS-DA analysis of E and Y human meibum samples. (**A**) An OPLS-DA scores plot of 21 Y and 29 E human meibum samples analyzed in a LC-MS experiment. (**B**) An OPLS-DA Hotelling's T2 Range plot of 21 Y and 29 E human meibum samples analyzed in a LC-MS experiment produced no strong outliers that would fall above the T2 Crit (95%) limit. (**C**) An S-Plot plot of 21 Y and 29 E human meibum samples produced no strong outliers that would fall above the T2 Crit (95%) limit. Compounds upregulated in E samples are located in the lower left quadrant, while compounds upregulated in Y samples are located in the upper right quadrant.

other hand, had noticeable p[1] values (i.e. rather high presence in meibum), but low p(Corr)[1] values, which suggested the low statistical significance of these observations.

Several variables with *m/z* values of 369.5562, 369.6544, 369.8233, and 369.8800 had the same retention times of 18.83 minutes as true CE with a characteristic *m/z* value of 369.3519, but their signal intensities were two orders of magnitude lower than those of CE, and, thus, were deemed to be experimental artifacts of the signal *m/z* 369.3519 and were excluded from the list of potential biomarkers, despite their noticeable impact on the S-plot.

The rest of variables demonstrated simultaneously low fold changes and high variances, regardless of the expression levels, which made them unlikely candidates for being biomarkers related to aging.

To verify these observations, the data were organized in tabulated format using a descriptive statistics feature of the EZinfo software package (Supplementary Table S2). A summary graph of 25 most prominent analytes in Y an E meibum samples is shown in Figure 4. Although there were several analytes observed that produced statistically significant differences with $P < 0.05$, they were on the lower end of the graph, with major species being expressed identically in both study groups.

A E versus Y scatter plot of all 393 analytes (see Fig. 4, insert) produced a straight line with $r^2 = 0.9994$ and no outliers, illustrating an extraordinary similarity of the two types of samples. Of a hundred most prominent variables with expression values of more than 0.5% of the most intense signal in both E and Y sample groups – *m/z* 369.3519 of CE – only 18 had a *P* value of better than 0.05. Among those 18 analytes, there were several major Chl-OAHFA (such as those with *m/z* values of 1116.0646, 1128.0671, 1142.0836, and 1156.0968), which spontaneously produced major OAHFA fragments *m/z* 747.7231, 759.7223, and 787.7535. Other Chl-OAHFA/OAHFA pairs either did not meet the $P < 0.05$ threshold, or their signals were too weak for quantitation (less than 0.5% of the major signal in the spectra).

Another group of lipids that differed between the Y and E groups were WE with *m/z* values of 631.638, 659.668, 671.669, 717.734, and 549.559. Importantly, these WE were present in the samples with relative abundances of <6.3% of the main peak, making them minor members of the WE family. At the same time, the expression levels of 21 major saturated and mono- and diunsaturated WE (SWE,

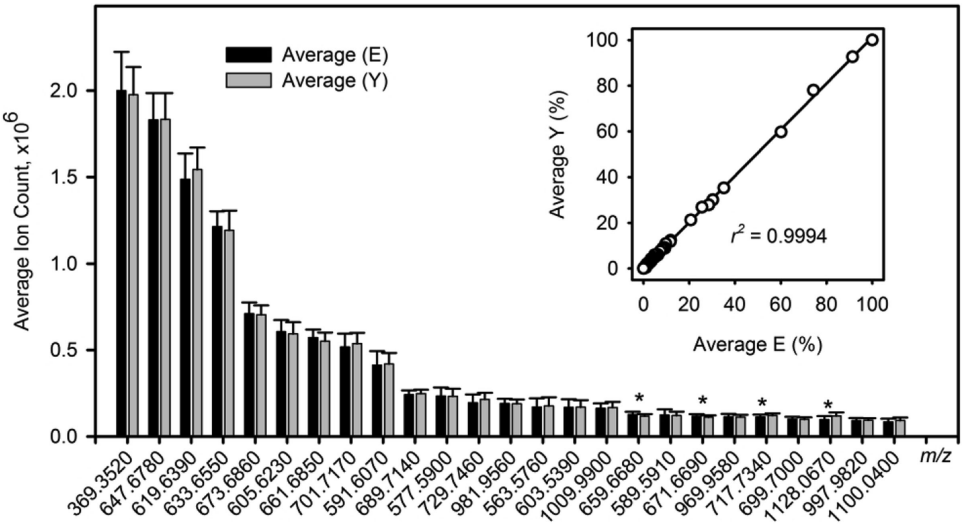

Figure 4. Targeted analysis of 25 major lipid analytes in E and Y human meibum samples. Lipids that differed between the E and Y samples with $P < 0.05$ are labeled with asterisks. *Insert*: A E vs. Y scatter plot for 393 compounds detected in Progenesis QI. Note the absence of outliers and a high r^2 value.

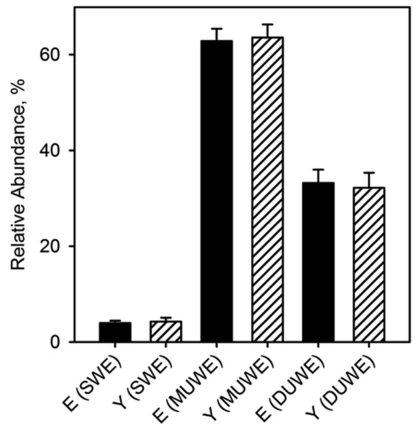

Figure 5. Comparison of degrees of meibomian WE unsaturation in E and Y study groups. Aggregate expression levels of saturated (SWE), monounsaturated (MUWE), and diunsaturated WE (DUWE) in Y and E human meibum samples are shown. The graph is based on apparent abundances of the analytes determined in direct LC-MS experiments. None of the groups produced any statistically significant differences with $P < 0.05$. The sum of SWE, MUWE, and DUWE for each study group equals 100%.

MUWE, and DUWE, correspondingly) of human meibum – *m/z* 563.5763, 565.5920, 577.5920, 579.6076, 591.6076, 593.6233, 603.6076, 605.6233, 607.6389, 617.6233, 619.6389, 621.6545, 631.6389, 633.6545, 635.6702, 645.6545, 647.6702, 649.6858, 659.6702, 661.6858, 663.7015, 673.6858, 701.7171, and 729.7484 – did not differ between the Y and E samples (Supplementary Table S2). An aggregate graph for various groups of WE (Fig. 5) illustrates our finding that their levels of expression were the same in both study groups.

Importantly, "relative abundance" of ions – a standard parameter that is used in mass spectrometry to describe the spectra – depends not only on the concentrations of the analytes of interest, but also on their ionization efficacy in given conditions and differs from class to class, or even from compound to compound within the same class. It makes it possible to calculate fold changes (or intersample differences) for specific compounds in different groups of samples, but may not accurately represent the true molar ratios of analytes of different types. Thus, we attempted a more targeted approach that utilized a set of chemical standards – SWE and MUWE – and compared them with matching meibomian WE. First, four pairs of SWE and MUWE with matching carbon chain lengths were analyzed in identical LC-MS conditions as an equimolar mixture, and their EIC were integrated to determine the LC-MS peak areas (Fig. 6A). Then, the SWE and MUWE matching pairs of the same carbon chain length were compared, and their peak area ratios were computed. It appeared that the LC-MS peak areas of all tested MUWE were consistently and substantially larger than those of matching equimolar SWE, with an average correction factor of times (11.9 ± 1.2) for all four pairs (Fig. 6B). This correction factor was applied to eight meibomian WE with the same *m/z* values as the WE standards, and the actual, corrected SWE/MUWE molar ratios were calculated and combined to produce Figure 6C. It was determined that the actual molar ratios of these eight WE did not differ between E and Y group enough to reach the level of statistical significance, and the overall SWE/MUWE balance was the same for both age groups. Last, aggregate SWE/MUWE ratios for E and Y samples were calculated (Fig. 6D) and the Student's *t*-test was performed. The difference between the study groups did not reach the level of statistical significance ($P = 0.185$). Therefore, no difference in the degrees of unsaturation of Meibomian WE between E and Y groups could be claimed.

Next, CE and Chl-OAHFA were analyzed using their common analytical fragment *m/z* 369.3519 and analyte-specific $(M + H)^+$ adducts. The EICs of the *m/z* 369.3519 fragment $(M - FA + H)^+$ produced 15 major chromatographic peaks of CE (Fig. 7A), whereas EIC of $(M + H)^+$ adducts – just one major peak per specific *m/z* and a few minor ones (Fig. 7B), which were identified on a case to case basis as isotopic peaks of related CE with different degrees of unsaturation, structural isomers of the major compound,

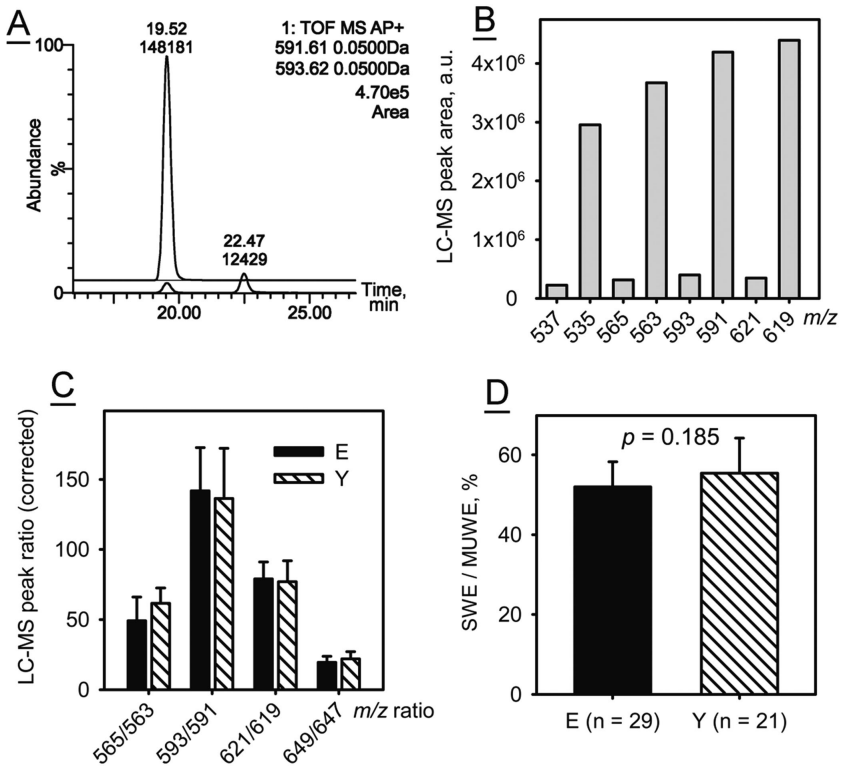

Figure 6. C_{18}-LC/APCI PIM MS analysis of wax esters. (**A**) Superimposed extracted ion chromatograms of WE ions *m/z* 591.61 ($C_{40}H_{79}O_2$; monounsaturated; upper trace) and *m/z* 593.62 ($C_{40}H_{81}O_2$; saturated; lower trace) obtained using a mixture of authentic chemical standards (50 µM each; injection volume 0.5 µL). Retention times (RT; in minutes) and peak areas (in arbitrary units) are shown at the tops of each peak. A small peak of the ion *m/z* 593.62 with a RT of around 19.52 min is produced by a third isotopic peak $(M + 2 + H)^+$ of the monounsaturated WE whose main $(M + H)^+$ has the same RT of 19.52 minutes. The second LC-MS peak with a RT of 22.47 min is the $(M + H)^+$ peak of the saturated WE. (**B**) LC-MS peak areas of eight authentic WE analyzed as an equimolar mixture. Note a much higher instrument response for monounsaturated WE. An average correction factor for all four pairs was calculated to be × 11.9 ± 1.2. (**C**) The LC-MS peak ratios for four matching pairs of saturated and unsaturated Meibomian WE. (**D**) Aggregate SWE/MUWE ratios for E and Y groups of subjects were computed for the same pairs of Meibomian WE. No statistically significant differences in their overall degrees of unsaturation were found.

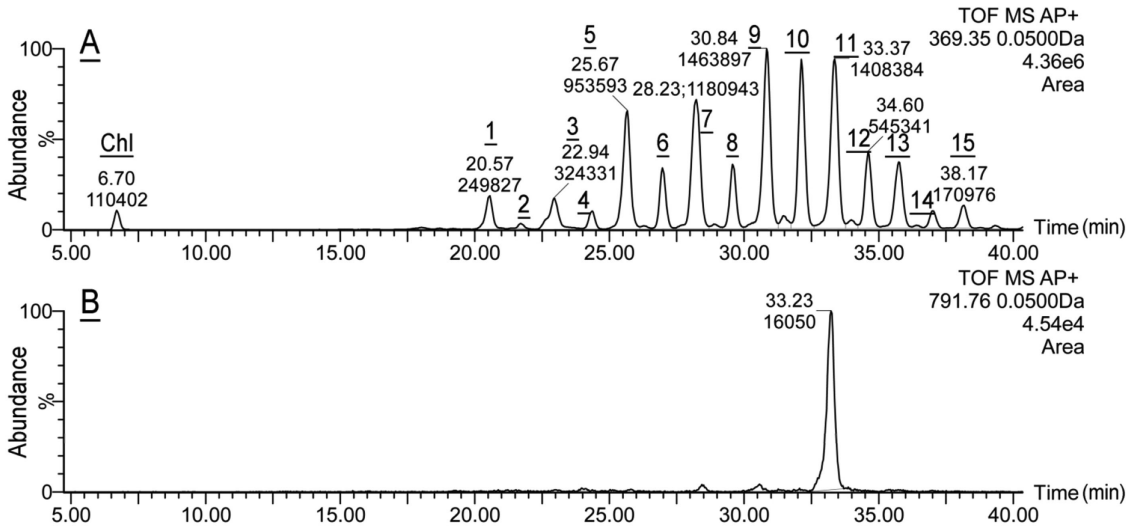

Figure 7. C_{18}-LC/APCI PIM MS analysis of cholesteryl esters of a representative human meibum sample. (**A**) Free cholesterol (Chl) and 15 cholesteryl esters peaks detected by monitoring ion *m/z* 369.3519. Peaks are labeled as Chl (free cholesterol) and 1 through 15 (CE). (**B**) Extracted ion chromatogram of a proton adduct of $C_{28:1}$-CE (*m/z* 791.7640).

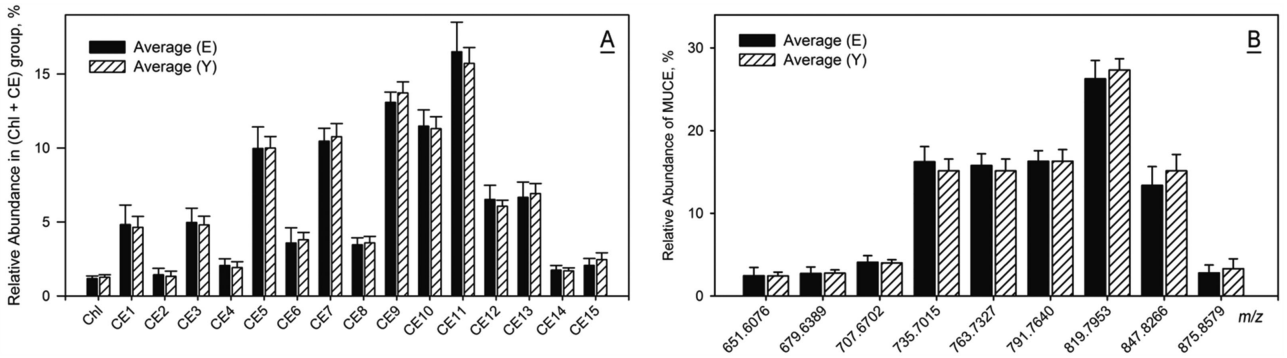

Figure 8. Targeted analysis of cholesteryl esters in E and Y human meibum samples. (**A**) Free cholesterol (Chl) and 15 cholesteryl esters peak areas obtained by integrating extracted ion chromatograms of ion *m/z* 369.3519. Peak numbers correspond to those in Figure 7A. (**B**) Peak areas calculated from $(M + H)^+$ extracted ion chromatograms of CE as illustrated in Figure 7B.

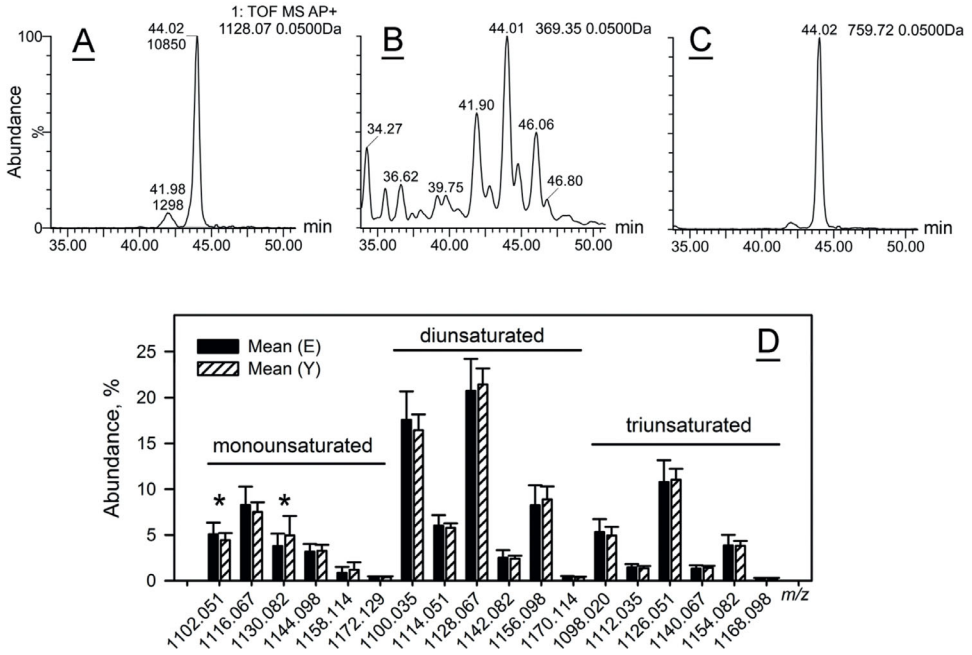

Figure 9. Targeted analysis of cholesteryl esters of OAHFA in E and Y human meibum samples. (**A**) Extracted ion chromatogram (EIC) of a $(M + H)^+$ adduct of Chl-OAHFA with *m/z* 1128.07. Other Chl-OAHFA were analyzed using the same approach. (**B**) EIC of a (M – OAHFA + $H)^+$ product ion *m/z* 369.35. (**C**) EIC of a (M – Chl + $H)^+$ product ion. (**D**) LC-MS peak areas were calculated from $(M + H)^+$ extracted ion chromatograms of eighteen major Chl-OAHFA. The only two analytes that differed between E and Y samples with $P < 0.05$ are labeled with asterisk (*). Saturated Chl-OAHFA were exceedingly minor components of the family in both age groups. Total sum of all abundances equals 100%.

or unrelated isobaric compounds. Integration of (M + H – FA)$^+$ and $(M + H)^+$ peaks revealed no statistically significant differences between E and Y study groups (Fig. 8A). Similar results were obtained upon analyzing nine major $(M + H)^+$ adducts of CE (Fig. 8B), with only two compounds being expressed at slightly different levels.

Major Chl-OAHFA, identified as potential biomarkers in the S-plot (see Fig. 3C), were analyzed in a similar fashion using integration of EIC of specific analytes (Fig. 9A). The analytes routinely produced more than one LC-MS peaks, such as two peaks shown in Figure 9A. The major peak with the retention time (RT) of 44.02 minutes was the true diunsaturated Chl-OAHFA with *m/z* 1128.0671, whereas the smaller peak with RT of 41.98 minutes was produced by a third isotopic peak $(M + H + 2)^+$ of a triunsaturated Chl-OAHFA with *m/z* 1126.0510. Thus, using C18-LC/APCI PIM MS provided a convenient way of baseline separation of these and similar lipid species, for their reliable quantitation. EIC of ions *m/z* 369.35 visualized the RT of (M – OAHFA + $H)^+$ adducts (characteristic of all Chl-OAHFA; Fig. 9B), whereas ion *m/z* 759.72 – of its (M – Chl + $H)^+$ fragment (Fig. 9C). After integration of EIC of all major (M + $H)^+$ LC-MS peaks, the following ratios of Chl-OAHFA was found (Fig. 9D). Importantly, only two compounds were found to be expressed at different levels which reached the threshold of $P < 0.05$. The rest of the compounds changed with no discernible pattern at statistically insignificant levels.

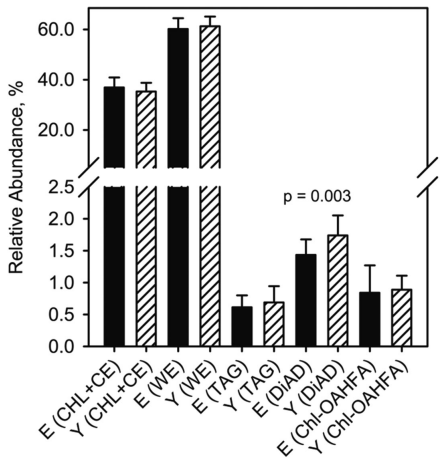

Figure 10. Targeted analysis of major lipid classes in E and Y human meibum samples conducted in LC-MS experiments in positive ion mode. Normalized data are shown. Total abundance within each group equals 100%. The only group of lipids that showed a statistically significant difference was DiAD ($P = 0.003$).

The effects of aging on polar lipids (cholesterol sulfate and OAHFA) were also studied, but revealed no statistically significant difference ($P = 0.405$) with an average standard deviation of ±21% of the mean values (not shown). Detailed analysis of these compounds is to be reported separately.

All major classes of lipids in E and Y samples that were detected in positive ion mode were compared groupwise (Fig. 10). Again, the samples demonstrated remarkable inter- and intragroup consistency, with the only group reaching the level of statistical significance being DiAD ($P = 0.003$). However, the difference in total DiAD between E and Y groups was rather small and DiAD themselves were a smaller group of lipids compared with WE and CE. No exact quantitation of DiAD was possible due to the lack of proper standards.

Finally, an attempt was made to associate meibomian lipid profiles of 36 Japanese subjects with their FBUT. The subjects were divided into 4 groups that differed in their FBUT times – (1) >5 seconds to <6 seconds; (2) ≥6 seconds to <8 seconds; (3) ≥8 seconds to <10 seconds; and (4) ≥10 seconds, and the meibum samples were analyzed using PCA-X approach (Fig. 11). All 393 analytes were included in the calculations. The analysis showed strongly overlapping groups with no clear clusters of samples, implying that the minor variations in the lipid composition of the samples described above had little effect on FBUT. Moreover, the values of FBUT for the Y group were 8.2 seconds ± 2.3 seconds (mean ± standard deviation; $n = 18$), whereas for the E group they were 7.9 seconds ± 2.9 seconds (n = 18). A very high P value of 0.7 indicated that there was no statistically significant difference in the FBUT between the study groups, according to the t-test.

Discussion

It has been reported that the aging is the contributing factor for the MGD.[1,42] With aging, MG change morphologically[26] and meibocyte differentiation decreases,[2] which presumably leads to quantitative and qualitative changes in meibomian lipid composition resulting in MGD.[43] In our current project, we focused primarily on the evaluation of the lipid composition of E and Y meibum samples, leaving other aspects of meibogenesis for future studies.

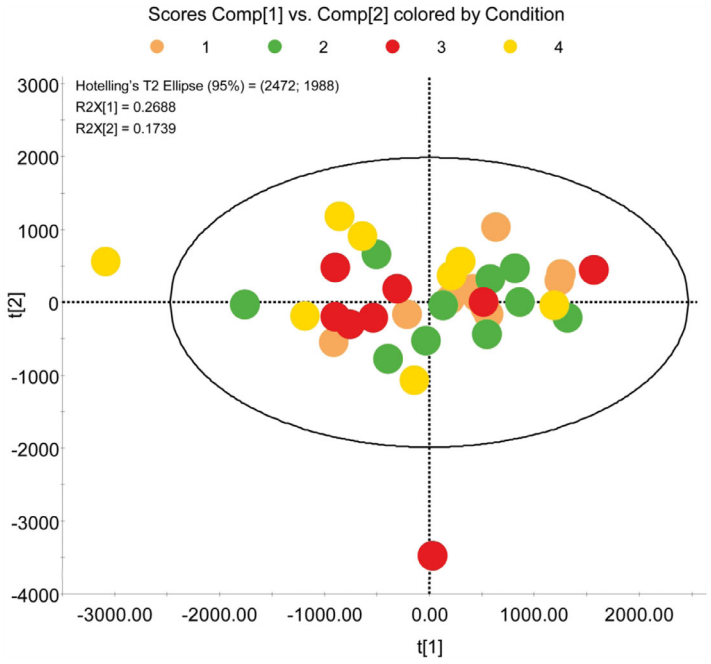

Figure 11. Untargeted PCA-X analysis of lipid profiles revealed no clear grouping of samples based on the subjects' FBUT times. The groups were as follows: group 1 – FBUT 6 seconds and below (*orange dots*; $n = 10$); group 2 – between 6 seconds and 8 seconds (*green dots*; $n = 10$); group 3 – between 8 seconds and 10 seconds (*red dots*; $n = 8$); group 4 – above 10 seconds (*yellow dots*; $n = 8$). Two outliers were detected in the latter group. Model used: dataset of 36 samples × 393 variables; Pareto scaling; no transformation applied; 2 components; variance explained – R2X(Cum), 44%.

Investigative Ophthalmology & Visual Science

Our data obtained for major meibomian lipids and lipid classes in LC-MS experiments showed no discernible differences between E and Y samples (see Figs. 4–10). Certain variations that were identified by PCA-X and OPLS-DA methods in, correspondingly, the Loading plot and S-plot (see Figs. 2, 3), such as changes in the ratios of some Chl-OAHFA, were statistically significant, but minimal (see Figs. 4, 9), and did not concern major lipid species. Thus, the physiological impact of those changes is expected to be rather small, if any.

We specifically evaluated the elongation patterns of major meibomian lipids, but did not observe any systematic changes between E and Y study groups: Their carbon chain lengths were identical, which contradicts earlier claims with regard to shortening the lipid carbon chains with aging. Similarly, no differences in the degree of unsaturation between E and Y samples (see Figs. 4–6, 8–10) were detected. As our study groups did not include infants and children, we could not verify earlier observations with regard to their meibomian lipids being longer and more saturated,[15] but no such effect was found in our 29 ± 5 and 68 ± 7 years old study groups.

As we have already reported when comparing meibum samples from Asians and Caucasians,[29] human[30] and mouse[44] males and females, pre- and post-treatment patients with DE,[45] and on other occasions, normal intersubject variability in the lipid composition of meibum for any study group was typically between 5% and 25% of the mean values for any given lipid (or ≤18%, on average, as shown in Supplementary Table S2), and was changing randomly with no specific pattern. Noticeable effects of race on composition of meibum that had been previously reported for Asians and Caucasians[46] were downplayed later on in a publication by the same team,[47] and proven to be virtually nonexistent in our recent publication.[29] Similarly, no noticeable effects of sex were observed for human[30] and mouse[44] meibum, although the menstrual cycle may have an impact on the overall fatty acid (FA) balance in human meibomian lipids.[48] The conclusion about high similarities between meibum samples from different donors is supported by our analysis of the gene expression profiles in MG of humans[30] and mice,[44] which showed only minor inter-donor variability.

Phospholipids and sphingomyelins – all being extremely minor components of meibum (typically, less than 0.1% of total lipid content[49]) – also varied from sample to sample, but variations in their presence should not have any measurable effect on the properties of the tear film as abnormal lipids should be present at much higher levels to induce noticeable changes in the rheological properties of meibum.[50–52]

The most variable groups in our hands were Chl and TAG (all minor groups in normal meibum), and DiAD and Chl-OAHFA (see Fig. 10). However, the fold changes in these lipids produced very close mean values and rather large standard deviation values for E and Y study groups, possibly implying the random nature of observed changes. Thus, only slight differences between young and old non-MGD/non-DE subjects were observed in our study, which, apparently, were too small to induce disruptive changes in ocular surface homeostasis and FBUT (see Fig. 11). It remains to be seen if these lipids – Chl, TAG, DiAD, and Chl-OAHFA – can be classified as true molecular biomarkers of MG aging, regardless of whether a minor decline in their amounts in meibum of elderly can actually have an impact on the tear film stability and the tear film breakup times.

It should be noted that in this study, some subjects showed FBUT between 6 seconds and 10 seconds, which indicated that those subjects had mild tear film instability,[53] although they did not meet the diagnostic criteria of DE (≤5 seconds). There was no significant difference in FBUT between young and elderly subjects (*t*-test: $P = 0.66$). Thus, the elderly subjects that were recruited for our study showed no apparent age-related DE: they only showed mild thinning and drop-out of MGs by meibography examination, but showed neither lid margin abnormalities nor obstruction of MG orifices and the meibo-score in the elderly was higher than that in young subjects, as previously reported (*t*-test: $P < 0.01$).

Our results support a growing understanding that chronological aging does not necessarily correlate with biological (also known as physiological or functional) aging, as no obvious decline/changes in quality of meibum was observed in the E group of human volunteers compared to the Y group, at least with regard to the detected lipid species. Importantly, in a recent study we established that dietary deuterated Chl (d-Chl) could be incorporated in mouse meibum as free compound as well as MG-type CE.[54] Moreover, the rate of d-Chl esterification in MG lagged behind the rate of its absorption from the blood, which led to a gradual accumulation of free d-Chl in MG. Thus, the diet, individual differences in lipid metabolism and transport caused by genetic/genomic factors, different comorbidities, and medication use may be alternative reasons for meibum variability and altered tear film stability reported in various studies, including those related to MGD and aging. Furthermore, a decline in the amount of available meibum due to MG atrophy and MG dropout, and its impeded delivery onto the ocular surface could be additional contributing factors to the tear film instability, which should be evaluated in future studies.

Acknowledgments

Supported by a National Institutes of Health grant R01 EY027349 (to I.A.B.) and grants from the Japanese Ministry of Education, Culture, Sports, Science and Technology (16K11295 and 19K09996, to T.S.)

Disclosure: **I.A. Butovich**, None; **T. Suzuki**, None

References

1. Hykin PG, Bron AJ. Age-related morphological changes in lid margin and meibomian gland anatomy. *Cornea*. 1992;11:334–342.
2. Nien CJ, Massei S, Lin G, et al. Effects of age and dysfunction on human meibomian glands. *Arch Ophthalmol*. 2011;129:462–469.
3. Wang MTM, Muntz A, Lim J, et al. Ageing and the natural history of dry eye disease: A prospective registry-based cross-sectional study. *Ocul Surf*. 2020;18:736–741.
4. Xiao J, Adil MY, Chen X, et al. Functional and Morphological Evaluation of Meibomian Glands in the Assessment of Meibomian Gland Dysfunction Subtype and Severity. *Am J Ophthalmol*. 2020;209:160–167.
5. Den S, Shimizu K, Ikeda T, Tsubota K, Shimmura S, Shimazaki J. Association between meibomian gland changes and aging, sex, or tear function. *Cornea*. 2006;25:651–655.
6. Goto E, Monden Y, Takano Y, et al. Treatment of non-inflamed obstructive meibomian gland dysfunction by

an infrared warm compression device. *Br J Ophthalmol*. 2002;86:1403–1407.
7. Eom Y, Choi KE, Kang SY, Lee HK, Kim HM, Song JS. Comparison of meibomian gland loss and expressed meibum grade between the upper and lower eyelids in patients with obstructive meibomian gland dysfunction. *Cornea*. 2014;33:448–452.
8. Eom Y, Na KS, Cho KJ, et al. Distribution and Characteristics of Meibomian Gland Dysfunction Subtypes: A Multicenter Study in South Korea. *Korean J Ophthalmol*. 2019;33:205–213.
9. Wojtowicz JC, Butovich IA, McMahon A, et al. Time-dependent degenerative transformations in the lipidome of chalazia. *Exp Eye Res*. 2014;127:261–269.
10. Nicolaides N, Flores A, Santos EC, Robin JB, Smith RE. The lipids of chalazia. *Invest Ophthalmol Vis Sci*. 1988;29:482–486.
11. Osae EA, Bullock T, Chintapalati M, et al. Obese Mice with Dyslipidemia Exhibit Meibomian Gland Hypertrophy and Alterations in Meibum Composition and Aqueous Tear Production. *Int J Mol Sci*. 2020;21:8772.
12. Fukuoka S, Arita R, Mizoguchi T, et al. Relation of Dietary Fatty Acids and Vitamin D to the Prevalence of Meibomian Gland Dysfunction in Japanese Adults: The Hirado-Takushima Study. *J Clin Med*. 2021;10:350.
13. Borchman D, Foulks GN, Yappert MC. Confirmation of changes in human meibum lipid infrared spectra with age using principal component analysis. *Curr Eye Res*. 2010;35:778–786.
14. Borchman D, Foulks GN, Yappert MC, et al. Physical changes in human meibum with age as measured by infrared spectroscopy. *Ophthalmic Res*. 2010;44:34–42.
15. Borchman D, Foulks GN, Yappert MC, Milliner SE. Differences in human meibum lipid composition with meibomian gland dysfunction using NMR and principal component analysis. *Invest Ophthalmol Vis Sci*. 2012;53:337–347.
16. Borchman D, Foulks GN, Yappert MC, Milliner SE. Changes in human meibum lipid composition with age using nuclear magnetic resonance spectroscopy. *Invest Ophthalmol Vis Sci*. 2012;53:475–482.
17. Borchman D, Yappert MC, Milliner SE, et al. 13C and 1H NMR ester region resonance assignments and the composition of human infant and child meibum. *Exp Eye Res*. 2013;112:151–159.
18. Shrestha RK, Borchman D, Foulks GN, Yappert MC, Milliner SE. Analysis of the composition of lipid in human meibum from normal infants, children, adolescents, adults, and adults with meibomian gland dysfunction using (1)H-NMR spectroscopy. *Invest Ophthalmol Vis Sci*. 2011;52:7350–7358.
19. Sledge S, Henry C, Borchman D, et al. Human Meibum Age, Lipid-Lipid Interactions and Lipid Saturation in Meibum from Infants. *Int J Mol Sci*. 2017;18:1862.
20. Benlloch-Navarro S, Franco I, Sanchez-Vallejo V, Silvestre D, Romero FJ, Miranda M. Lipid peroxidation is increased in tears from the elderly. *Exp Eye Res*. 2013;115:199–205.
21. Butovich IA. Meibomian glands, meibum, and meibogenesis. *Exp Eye Res*. 2017;163:2–16.
22. Butovich IA, McMahon A, Wojtowicz JC, Lin F, Mancini R, Itani K. Dissecting lipid metabolism in meibomian glands of humans and mice: An integrative study reveals a network of metabolic reactions not duplicated in other tissues. *Biochim Biophys Acta*. 2016;1861:538–553.
23. Sullivan BD, Evans JE, Dana MR, Sullivan DA. Influence of aging on the polar and neutral lipid profiles in human meibomian gland secretions. *Arch Ophthalmol*. 2006;124:1286–1292.
24. Amano S. Meibomian Gland Dysfunction: Recent Progress Worldwide and in Japan. *Invest Ophthalmol Vis Sci*. 2018;59:DES87–DES93.
25. Shimazaki J, Goto E, Ono M, Shimmura S, Tsubota K. Meibomian gland dysfunction in patients with Sjogren syndrome. *Ophthalmology*. 1998;105:1485–1488.
26. Arita R, Itoh K, Inoue K, Amano S. Noncontact infrared meibography to document age-related changes of the meibomian glands in a normal population. *Ophthalmology*. 2008;115:911–915.
27. Tsubota K, Yokoi N, Shimazaki J, et al. New Perspectives on Dry Eye Definition and Diagnosis: A Consensus Report by the Asia Dry Eye Society. *Ocul Surf*. 2017;15:65–76.
28. Butovich IA, Suzuki T. Delineating a novel metabolic high triglycerides-low waxes syndrome that affects lipid homeostasis in meibomian and sebaceous glands. *Exp Eye Res*. 2020;199:108189.
29. Butovich IA, Suzuki T, Wojtowicz J, Bhat N, Yuksel S. Comprehensive profiling of Asian and Caucasian meibomian gland secretions reveals similar lipidomic signatures regardless of ethnicity. *Sci Rep*. 2020;10:14510.
30. Butovich IA, Bhat N, Wojtowicz JC. Comparative Transcriptomic and Lipidomic Analyses of Human Male and Female Meibomian Glands Reveal Common Signature Genes of Meibogenesis. *Int J Mol Sci*. 2019;20:4539.
31. Nicolaides N, Kaitaranta JK, Rawdah TN, Macy JI, Boswell FM, 3rd, Smith RE. Meibomian gland studies: comparison of steer and human lipids. *Invest Ophthalmol Vis Sci*. 1981;20:522–536.
32. Butovich IA. The Meibomian puzzle: combining pieces together. *Prog Retin Eye Res*. 2009;28:483–498.
33. Butovich IA. Tear film lipids. *Exp Eye Res*. 2013;117:4–27.
34. Butovich IA. Lipidomics of human Meibomian gland secretions: Chemistry, biophysics, and physiological role of Meibomian lipids. *Prog Lipid Res*. 2011;50:278–301.
35. Pucker AD, Nichols JJ. Analysis of meibum and tear lipids. *Ocul Surf*. 2012;10:230–250.
36. Pucker AD, Haworth KM. The presence and significance of polar meibum and tear lipids. *Ocul Surf*. 2015;13:26–42.
37. Tiffany JM. The lipid secretion of the meibomian glands. *Adv Lipid Res*. 1987;22:1–62.
38. Butovich IA, Borowiak AM, Eule JC. Comparative HPLC-MS analysis of canine and human meibomian lipidomes: many similarities, a few differences. *Sci Rep*. 2011;1:24.
39. Butovich IA, Lu H, McMahon A, Eule JC. Toward an animal model of the human tear film: biochemical comparison of the mouse, canine, rabbit, and human meibomian lipidomes. *Invest Ophthalmol Vis Sci*. 2012;53:6881–6896.
40. Chen J, Green-Church KB, Nichols KK. Shotgun lipidomic analysis of human meibomian gland secretions with electrospray ionization tandem mass spectrometry. *Invest Ophthalmol Vis Sci*. 2010;51:6220–6231.
41. Butovich IA, Uchiyama E, McCulley JP. Lipids of human meibum: mass-spectrometric analysis and structural elucidation. *J Lipid Res*. 2007;48:2220–2235.
42. Hom MM, Martinson JR, Knapp LL, Paugh JR. Prevalence of Meibomian gland dysfunction. *Optom Vis Sci*. 1990;67:710–712.
43. Nichols KK, Foulks GN, Bron AJ, et al. The international workshop on meibomian gland dysfunction: executive summary. *Invest Ophthalmol Vis Sci*. 2011;52:1922–1929.
44. Butovich IA, McMahon A, Wojtowicz JC, Bhat N, Wilkerson A. Effects of sex (or lack thereof) on meibogenesis in mice (Mus musculus): Comparative evaluation of lipidomes and transcriptomes of male and female tarsal plates. *Ocul Surf*. 2019;17:793–808.

Investigative Ophthalmology & Visual Science

45. Wojtowicz JC, Butovich I, Uchiyama E, Aronowicz J, Agee S, McCulley JP. Pilot, prospective, randomized, double-masked, placebo-controlled clinical trial of an omega-3 supplement for dry eye. *Cornea*. 2011;30:308–314.
46. Lam SM, Tong L, Yong SS, et al. Meibum lipid composition in Asians with dry eye disease. *PLoS One*. 2011;6:e24339.
47. Lam SM, Tong L, Duan X, Petznick A, Wenk MR, Shui G. Extensive characterization of human tear fluid collected using different techniques unravels the presence of novel lipid amphiphiles. *J Lipid Res*. 2014;55:289–298.
48. Suzuki T, Fujiwara S, Kinoshita S, Butovich IA. Cyclic Change of Fatty Acid Composition in Meibum During the Menstrual Cycle. *Invest Ophthalmol Vis Sci*. 2019;60:1724–1733.
49. Butovich IA, Uchiyama E, Di Pascuale MA, McCulley JP. Liquid chromatography-mass spectrometric analysis of lipids present in human meibomian gland secretions. *Lipids*. 2007;42:765–776.
50. Arciniega JC, Nadji EJ, Butovich IA. Effects of free fatty acids on meibomian lipid films. *Exp Eye Res*. 2011;93:452–459.
51. Arciniega JC, Uchiyama E, Butovich IA. Disruption and destabilization of meibomian lipid films caused by increasing amounts of ceramides and cholesterol. *Invest Ophthalmol Vis Sci*. 2013;54:1352–1360.
52. Yoshida M, Yamaguchi M, Sato A, Tabuchi N, Kon R, Iimura KI. Role of Endogenous Ingredients in Meibum and Film Structures on Stability of the Tear Film Lipid Layer against Lateral Compression. *Langmuir*. 2019;35:8445–8451.
53. Tsubota K, Pflugfelder SC, Liu Z, et al. Defining Dry Eye from a Clinical Perspective. *Int J Mol Sci*. 2020;21:9271.
54. Butovich IA, Wilkerson A, Yuksel S. Differential effects of dietary cholesterol and triglycerides on the lipid homeostasis in Meibomian glands. *J Steroid Biochem Mol Biol*. 2021;211:105894.

Investigative Ophthalmology & Visual Science